

# Nature of the giant magnetostriction strains in single-crystal alloys of terbium with yttrium and gadolinium

S. A. Nikitin

Moscow State University

(Submitted 8 April 1980)

Zh. Eksp. Teor. Fiz. **80**, 207–213 (January 1981)

Field-induced and spontaneous magnetostriction in single-crystal terbium–yttrium and terbium–gadolinium alloys is investigated experimentally. It is established that the dependence of the giant magnetostriction in the basal plane on the magnetization and on the temperature can be described by a relation that follows from the theory for the single-ion magnetocrystalline interaction. The magnetization dependence of the giant magnetostriction along the hexagonal axis, which accompanies the destruction of the helicoidal magnetic structure in a magnetic field  $H > H_{cr}$ , indicates that this magnetostriction is due to a change of the exchange energy and of the electron structure at  $H = H_{cr}$ . It is shown that the spontaneous magnetostriction of terbium and its alloys receive, beside the exchange contribution, also an appreciable contribution due to the single-ion magnetocrystalline interaction.

PACS numbers: 75.80. + q

The anomalously high magnetostriction of rare-earth metals (REM) and their alloys and compounds can at present be explained by the microscopic theory<sup>1,2</sup> only qualitatively. To assess the contributions of the various interaction of the giant magnetostriction ( $\lambda > 10^{-3}$ ) of REM alloys we have investigated jointly the magnetostriction and magnetization as functions of the temperature and of the magnetic field in terbium–yttrium and terbium–gadolinium alloys.

The magnetization was measured with a vibration magnetometer (with accuracy 3%). The magnetostriction was measured by the strain-gauge method (accuracy to 3%). A magnetic field up to 65 kOe was produced by a superconducting solenoid. The preparation of the alloy single crystals and the control of their quality were described in detail earlier.<sup>3</sup>

Giant magnetostriction in the ferromagnetic state is observed in heavy REM and their alloys in a field applied to the basal plane when it is measured along the axes  $a$  and  $b$ , which also lie in this plane.

Figure 1 shows the temperature dependence of the saturation magnetostriction  $\lambda_s(b, c)$ ,  $\lambda_s(b, b)$ , and  $\lambda_s(a, b)$  of a single crystal of  $Tb_{0.5}Ge_{0.5}$  (here and elsewhere, the first index in the parentheses designates the direction of the magnetic field, and the second the measurement direction). It is seen from Fig. 1 that at 4.2 K the values of  $\lambda_s(b, b)$  and  $\lambda_s(a, b)$  exceed  $1.5 \times 10^{-3}$ , with  $\lambda_s(b, b) > 0$  and  $\lambda_s(a, b) < 0$ . When the temperature is raised and the Curie point  $\Theta = 261$  K is approached, these values decrease monotonically to zero. The magnetostriction  $\lambda_s(b, c)$  along the  $c$  axis at  $H \parallel b$  is relatively small, and an observable increase is observed only near  $\Theta$  as a result of the para-process. It follows also from the experimental data that  $\lambda_s(a, a) > 0$  and  $\lambda_s(b, a) < 0$ . Thus, if the measurement and magnetic-field directions coincide in the basal plane then the magnetostriction is positive, and if they do not coincide it is negative.

This experimental fact can be described by a relation that is a particular case of a formula obtained by group theory when account is taken of the magnetic and crys-

tallographic symmetry,<sup>2</sup> namely, the magnetostriction induced by a field  $H \parallel b \parallel I_s$  ( $H$  exceeds the saturation field) along the  $b$  axis of a single-domain hexagonal crystal is equal to

$$\lambda_s(b, b) = \lambda^{\gamma, 2} \sin^2 \psi, \quad (1)$$

while for  $H \parallel a \parallel I_s$  we have

$$\lambda_s(a, b) = -\lambda^{\gamma, 2} \cos^2 \psi, \quad (2)$$

where  $\lambda^{\gamma, 2}$  is the magnetostriction constant, and  $\psi$  is the angle between the spontaneous magnetization vector  $I_s$  in a single-domain crystal and the easy magnetization axis (EMA) along the  $b$  axis (the angle between the axes  $a$  and  $b$  is  $\beta = 30^\circ + 60^\circ n$ , where  $n = 0, 1, 2, 3, 4, 5$ ).

It follows from (1) that in a single-domain crystal with the EMA along the  $b$  axis the magnetostriction  $\lambda_s(b, b) = 0$ . The fact that experiment yields  $\lambda_s(b, b) \neq 0$  (Fig. 1) must be attributed to the presence of a domain structure in the crystal.

An hexagonal crystal with an easy magnetization plane has three EMA and six domain magnetic-moment directions, so that if all the domains are equal in volume the field-induced magnetostriction along one of the direc-

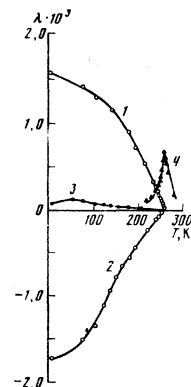


FIG. 1. Temperature dependences of the saturation magnetostriction: 1)  $\lambda_s(b, b)$ , 2)  $\lambda_s(a, b)$ , 3)  $\lambda_s(b, c)$ , as well as of the magnetostriction  $\lambda_H(b, c)$  (curve 4) in a field  $H = 14.5$  kOe for single-crystal  $Tb_{0.5}Gd_{0.5}$ .

tions of type  $b$  is

$$\lambda(b, b) = \frac{1}{6} \sum_{i=1}^6 \lambda^{i,2} \sin^2 \psi_i, \quad (3)$$

where  $\psi_i$  runs through the values  $60^\circ n$  ( $n = 0, 1, 2, 3, 4, 5$ ). Substituting these values in (3) and summing, we obtain the saturation magnetostriction of a crystal with a domain structure:

$$\lambda_s(b, b) = \lambda^{i,2}/2.$$

The saturation magnetostriction of a multidomain crystal along the  $b$  axis with the field applied along the  $a$  axis can be found in similar fashion:

$$\lambda_s(a, b) = -\lambda^{i,2}/2.$$

Consequently, at  $\lambda^{i,2} > 0$  we have  $\lambda_s(b, b) > 0$  and  $\lambda_s(a, b) < 0$ , which agrees with experiment (see Fig. 1).

Unequal absolute values of  $\lambda_s(b, b)$  and  $\lambda_s(a, b)$  are observed in experiment because in real crystals the domains are not strictly statistically distributed along the six equally probable magnetization orientations. This can be caused by even negligible defects and internal stresses in the crystals in the course of their growth, or can occur when the samples are cut.

To assess the nature of the field-induced giant magnetization in the basal plane,  $\lambda(b, b)$  and  $\lambda(a, b)$ , we consider the temperature dependence of the magnetostriction constant  $\lambda^{i,2}$ , which is independent of the initial domain distribution and describes orthorhombic distortions in the basal plane:

$$\lambda^{i,2} = \lambda_s(b, b) - \lambda_s(a, b). \quad (4)$$

Figure 2 shows the dependence of  $\lambda^{i,2}$  on the relative magnetization  $m_{Tb}$  of the terbium sublattice for the alloys  $Tb_x Y_{1-x}$  and  $Tb_x Gd_{1-x}$ . In  $Tb_x Gd_{1-x}$  the value of  $m_{Tb}$  was obtained by solving the molecular-field equations<sup>4</sup> for the magnetization, using the previously obtained<sup>5</sup> values of the exchange integrals. To construct the  $\lambda^{i,2}(m_{Tb})$  plot we used magnetostriction and magnetiza-

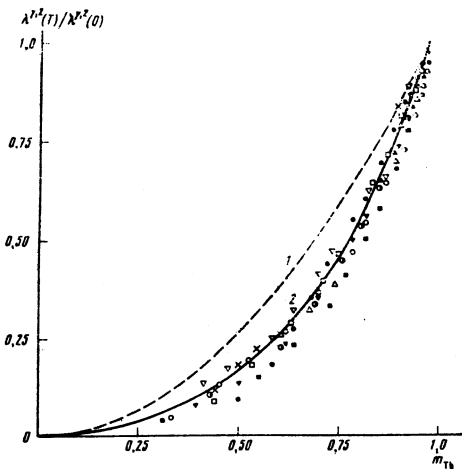


FIG. 2. Relative values of the magnetostriction constant  $\lambda^{i,2}(T)/\lambda^{i,2}(0)$  vs. the relative magnetization  $m_{Tb}$  for  $Tb_x Gd_{1-x}$  alloys with different values of  $x$ . ( $\circ$ )  $x = 0.09$ ; ( $\bullet$ )  $0.20$ , ( $\square$ )  $0.39$ , ( $\times$ )  $0.50$ ; ( $\nabla$ )  $0.70$ ; ( $\blacksquare$ )  $0.94$ , and for  $Tb_x Y_{1-x}$  alloys with; ( $\triangle$ )  $x = 1$ ; ( $\Delta$ )  $0.91$ , ( $\nabla$ )  $0.835$ , ( $\triangle$ )  $0.50$ . Curves 1 and 2 were obtained from formulas (6) and (5), respectively.

tion values measured in a wide temperature range, from 4.2 K to the points of the phase transitions from the magnetically ordered into the paramagnetic state.

The solid line (curve 2) of Fig. 2 is plotted in accord with a formula obtained in the theory<sup>2</sup> by taking into account the strain dependence of the single-ion magneto-crystalline interaction:

$$\lambda^{i,2}(T)/\lambda^{i,2}(0) = I_{5/2}[L^{-1}(m_{Tb})], \quad (5)$$

where  $\lambda^{i,2}(0)$  is the value of the constant at 0 K,  $\hat{I}_{5/2}(x)$  is the ratio of the hyperbolic Bessel function of order 5/2 to the hyperbolic function of order 1/2, and  $L^{-1}(m_{Tb})$  is the inverse of the Langevin function  $L(x) = \hat{I}_{3/2}(x)$ .

In the wide temperature interval  $1 > m > 0.5$  we have

$$I_{5/2}[L^{-1}(m)] \sim m^2.$$

The dashed line in Fig. 2 corresponds to the relation expected for the exchange mechanism:

$$\lambda^{i,2}(T)/\lambda^{i,2}(0) = m_{Tb}^2. \quad (6)$$

It is seen from Fig. 2 that in these alloys  $\lambda^{i,2}$  has the magnetization dependence expected for single-ion contributions [relation (5)]. This allows us to conclude that the giant magnetostriction in the basal plane is due to the interaction of the orbital angular momentum of the  $4f$  subshell of the rare-earth ion with the crystal lattice field.

In the antiferromagnetic  $Tb_x Y_{1-x}$  alloys one observes besides the magnetostriction in the basal plane also a giant magnetostriction of another type, namely magnetostriction directed along the hexagonal axis and accompanying the destruction of the antiferromagnetic helicoidal structure in these alloys in magnetic fields  $H > H_{cr}$ . At  $H < H_{cr}$  this magnetostriction is small, but at  $H > H_{cr}$  it increases abruptly and reaches  $\lambda \sim 10^{-3}$  at low temperatures. This can be seen in Fig. 3, which shows the isotherms of the magnetostriction  $\lambda(b, c)$  measured in a field  $H \parallel b$  along the  $c$  axis for a  $Tb_{0.63} Y_{0.37}$  single crystal in which, according to neutron-diffraction<sup>6</sup> and magnetic<sup>7</sup> investigations, a helicoidal magnetic structure exists below the antiferromagnetism-paramagnetism transition point  $\Theta_2$ . The  $\lambda(H)$  isotherms exhibit near  $H_{cr}$  a noticeable hysteresis when the magnetic field is increased and decreased. This indicates that the phase transition at  $H = H_{cr}$  is of first order. The width of the hysteresis loop increases strongly with decreasing temperature. There is prac-

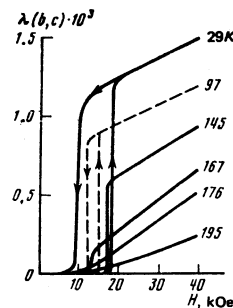


FIG. 3. Isotherms of magnetostriction  $\lambda(b, c)$  of single-crystal  $Tb_{0.63} Y_{0.37}$ .

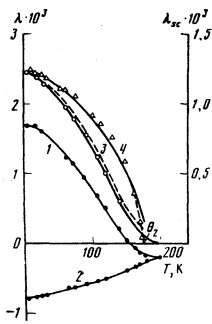


FIG. 4. Temperature dependences of the saturation magnetostrictions  $\lambda_b$  ( $b$ ,  $b$ ) (curve 1) and  $\lambda_a$  ( $a$ ,  $b$ ) (curve 2) of  $Tb_{0.63}Y_{0.37}$  and of the magnetostriction constant  $\lambda^{\nu,2}$  (3) helicoidal magnetostriction  $\lambda_{sc}$  (4) at  $H > H_{cr}$ . The dashed curve was calculated from formula (5). The curve drawn through the experimental  $\lambda_{sc}$  points was calculated from the formula  $\lambda_{sc} = \lambda_{sc}(0) m^2$ .

tically no hysteresis near  $\Theta_2$ .

The jump of the magnetostriction along the  $c$  axis at  $H = H_{cr}$  will be called here "helicoidal" magnetostriction and will be designated  $\lambda_{sc}$ . It turns out that in  $Tb_xY_{1-x}$  alloys  $\lambda_{sc}$  is proportional to the square of the spontaneous magnetization in a wide temperature interval (Fig. 4), in contrast to the constant  $\lambda^{\nu,2}$ , which can be described by relation (5).

A proportionality of the magnetostriction constants to the square of the spontaneous magnetization is expected, as noted above, for the exchange mechanism. It can therefore be concluded that the helicoidal magnetostriction along the  $c$  axis is due to the change of the energy of the two-ion exchange interaction between the magnetic layers and to the change of the energy spectrum of the conduction electrons in the antiferromagnetism-ferromagnetism transition at  $H > H_{cr}$ .<sup>8</sup>

The Callens' theory<sup>2</sup> leads, under certain assumptions for the low-temperature region  $1 > m > 0.5$ , to relations that describe the magnetization dependence of the spontaneous magnetization  $\Lambda$  along the crystallographic axes  $b$ ,  $a$ , and  $c$ :

$$\Lambda_b/m^2 = \lambda_1^{\alpha,0} + \lambda_0 m, \quad (7)$$

$$\Lambda_a/m^2 = \lambda_1^{\alpha,0} + (\lambda_0 - \lambda^{\nu,2}) m, \quad (8)$$

$$\Lambda_c/m^2 = \lambda_2^{\alpha,0} - \lambda_2^{\alpha,2} m/3, \quad (9)$$

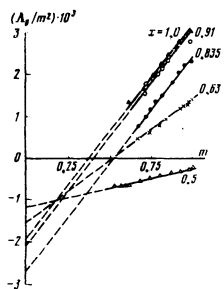


FIG. 5. Dependences of the spontaneous magnetostriction  $\Lambda_b$  divided by the square of the relative saturation magnetization  $m$  on the value of  $m$  for  $Tb_xY_{1-x}$  at different values of  $x$ .

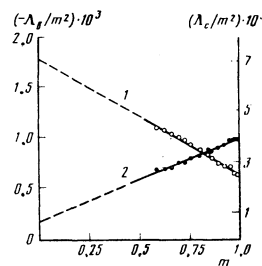


FIG. 6. Dependences of  $\Lambda_c/m^2$  (1) and  $\Lambda_b/m^2$  (2) on the relative saturation magnetization  $m$  for the alloy  $Tb_{0.5}Gd_{0.5}$ .

where

$$\lambda_0 = -\lambda_1^{\alpha,2}/3 + \lambda^{\nu,2}/2. \quad (10)$$

It is assumed here that the EMA is the  $b$  axis, and the magnetostriction constants  $\lambda^{\nu,2}$ ,  $\lambda_1^{\alpha,2}$ , and  $\lambda_2^{\alpha,2}$  are determined by the one-ion magnetocrystalline interaction. It follows from the theory<sup>2</sup> that  $\lambda_1^{\alpha,0}$  and  $\lambda_2^{\alpha,0}$  stem from the two-ion exchange terms of the Hamiltonian and describe the strain, which depends only on the magnitude of the magnetization and not on its direction.

Using the magnetostriction contributions to the thermal expansion, which we determined experimentally by a previously proposed<sup>9</sup> method, and which coincide with the spontaneous magnetization at  $m > 0.5$ , as well as the spontaneous magnetization  $I_s(T)$  obtained from the magnetization curves, we plotted the functions  $\Lambda_b/m^2$  and  $\Lambda_c/m^2$  against the relative magnetization  $m = I_s(T)/I_s(0)$  for terbium-yttrium alloys and for the alloy  $Tb_{0.5}Gd_{0.5}$ .

It is seen from Figs. 5 and 6 that the  $\Lambda_b/m^2 = f(m)$  and  $\Lambda_c/m^2 = \varphi(m)$  curves have linear sections, as expected on the basis of Eqs. (7)–(9). The intercepts of the lines  $\Lambda_b/m^2 = f(m)$  and  $\Lambda_c/m^2 = \varphi(m)$  on the ordinate axis are equal to  $\lambda_1^{\alpha,0}$  and  $\lambda_2^{\alpha,0}$ , and the slopes amount respectively to  $\lambda_0$  and  $\lambda_2^{\alpha,2}/3$  for each straight line.

Having determined  $\lambda_1^{\alpha,0}$ ,  $\lambda_2^{\alpha,0}$ ,  $\lambda_0$ , and  $\lambda_2^{\alpha,2}$ , in this manner we can easily find  $\lambda^{\nu,2}$  if we substitute the experimentally determined  $\lambda^{\nu,2}$  in formula (10). The calculated magnetostriction constants for the alloys  $Tb_xY_{1-x}$  and  $Tb_{0.5}Gd_{0.5}$  are listed in Tables I and II. The tables show also the magnetostriction constants obtained for Gd and Dy by the same method from the previously published<sup>9</sup> experimental data.

The plots of Figs. 5 and 6 were obtained using the spontaneous magnetostriction and magnetization values measured for the same single crystals in a magnetic field stronger than both the saturation field and  $H_{cr}$  (for the antiferromagnetic alloys  $Tb_xY_{1-x}$  and Dy).

It follows from Table II that the magnetostriction con-

TABLE I. Magnetostriction constants and contributions to the spontaneous magnetostriction of  $Tb_xY_{1-x}$  alloys at 4.2 K.

$x$	along the $c$ axis		along the $b$ axis		along the $a$ axis	
	$\lambda_2^{\alpha,0} \cdot 10^3$	$-\lambda_2^{\alpha,2} \cdot 10^3$	$\lambda_1^{\alpha,0} \cdot 10^3$	$\lambda_0 \cdot 10^3$	$(\lambda_0 - \lambda^{\nu,2}) \cdot 10^3$	$\lambda^{\nu,2} \cdot 10^3$
1						
0.91	6.7	-4.3	-1.9	5.1	-0.36	5.46
0.835	10	-6	-2.4	5.2	0.1	5.1
0.83	14	-6	-2.7	5.1	0.74	4.36
0.63	8	-4.7	-1.5	2.9	0.44	2.46
0.50	6.1	-4	-1.2	0.98	0.87	1.85

TABLE II. Magnetostriction constants of Gd, Dy, and Tb<sub>0.5</sub>Gd<sub>0.5</sub> at 4.2 K.

Composition	$\lambda_1^{\alpha,0 \cdot 10^3}$	$\lambda_1^{\alpha,2 \cdot 10^3}$	$\lambda_2^{\alpha,0 \cdot 10^3}$	$\lambda_2^{\alpha,2 \cdot 10^3}$
Gd	-0.45 -0.43 [10]	-	4.26 7.61 [10]	-
Dy	-6.1 -4.3 [10]	-14 -9.1 [10]	11 12.9 [10]	10 10 [11]
Tb <sub>0.5</sub> Gd <sub>0.5</sub>	-0.17	-8.4	7.1	14

stants  $\lambda_1^{\alpha,1}$  and  $\lambda_2^{\alpha,2}$  obtained for REM by other methods<sup>10,11</sup> are in fair agreement with those obtained in the present study. This important circumstance verifies the method proposed by us for the determination of the magnetostriction constants.

It is seen from Table II that in Gd the exchange contributions to the spontaneous magnetostriction  $\lambda_2^{\alpha,0}$  and  $\lambda_1^{\alpha,0}$  [Eqs. (7)–(9)] exceed by an order of magnitude and more the one-ion contributions  $\lambda_8$  and  $-\lambda_2^{\alpha,2}/3$ . This can be attributed to the absence of the orbital angular momentum ( $L=0$ ) and to the sphericity of the electron 4f subshell in the ground state of the Gd<sup>3+</sup> ion.<sup>1</sup>

The spontaneous magnetostrictions of Tb, Dy, Tb<sub>x</sub>Y<sub>1-x</sub>, and Tb<sub>0.5</sub>Gd<sub>0.5</sub> along the c axis contain, besides the positive exchange contribution  $\lambda_2^{\alpha,0}$ , also a noticeable negative one-ion contribution  $-\lambda_2^{\alpha,2}/3$ . The exchange interaction expands and the one-ion magnetocrystalline interaction contracts the lattice parameter c. Since  $\lambda_2^{\alpha,0} > \lambda_2^{\alpha,2}/3$ , the exchange contribution predominates here, and expansion along the c axis is observed as a result. In spontaneous magnetostriction along the EMA, on the contrary, the positive one-ion contribution  $\lambda_6$  exceeds in absolute value the negative exchange contribution  $\lambda_1^{\alpha,0}$ , as a result of which expansion is observed also along the EMA.

The exchange interaction produces the same change of the dimensions of  $\lambda_1^{\alpha,0}$  along the axes a and b, so that the crystal symmetry is preserved. The one-ion magnetocrystalline interaction alters the circular symmetry in the basal plane, since it leads to unequal changes of

the dimension along and across the EMA. This change equals  $\lambda_6$  along the b axis and  $\lambda_6 - \lambda_7^2$  along the a axis, as follows from Eqs. (7)–(9). It is seen from Table I that these contributions are not equal, therefore orthorhombic distortions take place in the basal plane.

The reasons for the presence in the spontaneous magnetostriction of Tb, Dy, and their alloys of an appreciable contribution due to the one-ion magnetocrystalline interaction are that the ions Tb<sup>3+</sup> and Dy<sup>3+</sup> have an orbital angular momentum  $L \neq 0$  and that these ions have an asymmetric distribution of the electron density in the 4f subshell.

In conclusion, we are grateful to K. P. Belov for a discussion of the results, to N. P. Arutyunyan and V. P. Posyado for help with the work, and to G. E. Chuprikov for supplying the alloy single crystals.

<sup>1</sup>K. P. Belov, Vestnik MGU No. 5, 23 (1967).

<sup>2</sup>E. Callen and H. Callen, Phys. Rev. **139**, 455 (1965).

<sup>3</sup>V. P. Posyado, M. L. Grachev, and G. E. Chuprikov, Izv. AN SSSR, Metall, No. 3, 92 (1978).

<sup>4</sup>R. Z. Levitin, T. M. Perekalina, L. P. Shlyakhina, O. D. Chistyakov, and V. L. Yakovenko, Zh. Eksp. Teor. Fiz. **63**, 1401 (1972) [Sov. Phys. JETP **36**, 742 (1973)].

<sup>5</sup>S. A. Nikitin and N. P. Arutyunyan, Zh. Eksp. Teor. Fiz. **77**, 2018 (1979) [Sov. Phys. JETP **50**, 962 (1979)].

<sup>6</sup>H. Child, W. Koehler, E. Wollan, and J. Cable, Phys. Rev. **138**, 1655 (1965).

<sup>7</sup>S. A. Nikitin, Zh. Eksp. Teor. Fiz. **77**, 343 (1979) [Sov. Phys. JETP **50**, 176 (1979)].

<sup>8</sup>I. E. Dzyaloshinskii, Zh. Eksp. Teor. Fiz. **47**, 336 (1964) [Sov. Phys. JETP **20**, 223 (1965)].

<sup>9</sup>S. A. Nikitin, D. Kim, and O. D. Chistyakov, Zh. Eksp. Teor. Fiz. **71**, 1610 (1976) [Sov. Phys. JETP **44**, 843 (1976)].

<sup>10</sup>H. Bartolin, transl. in: Redkozemel'nye metally, splavy i soedineniya (Rare Earth Metals, Alloys, and Compound), Nauka, 1973, p. 125.

<sup>11</sup>V. L. Yakovenko, Author's abstract of candidates' dissertation, Phys Inst. Siberian Div. USSR Acad. Sciences, Krasnoyarsk, 1973.

Translated by J. G. Adashko